

Diffraction of short X-ray pulses in the general asymmetric Laue case – an analytic treatment

C. Malgrange^a and W. Graeff^{b*}

^aLaboratoire de Minéralogie-Cristallographie, Universités Paris 6 et Paris 7, Associé au CNRS, Case 115, 4 Place Jussieu, 75252 Paris CEDEX 05, France, and ^bHamburger Synchrotronstrahlungslabor HASYLAB am Deutschen Elektronensynchrotron DESY, Notkestrasse 85, 22603 Hamburg, Germany. E-mail: graeff@desy.de

After briefly describing the concept of short X-ray pulses (δ -function), the diffraction of such a short pulse by a crystal in the asymmetric Laue case is given. The results of the dynamical theory are adopted and an analytic result for the intensity distribution behind the crystal in the diffracted direction as well as in the forward direction is given and discussed in detail. The incoming δ pulse is no longer infinitely short but shows a pronounced structure over a limited temporal or spatial region which is connected to the well known Pendellösung effect. Also the limitations of these findings are critically inspected.

Keywords: free-electron lasers; X-ray optics; X-ray pulses; dynamical diffraction.

1. Introduction

The free-electron laser (FEL) is expected to become an extraordinary source of X-rays. This has resulted in at least two projects promising to deliver photons with X-ray energies, namely the TESLA project at DESY (DESY, 1997, 2001) and SLAC (SLAC, 1998). However, the X-ray beams coming out of such a FEL have a rather special time structure.

At TESLA-XFEL a bunch train of electrons is released at a repetition rate of 5–10 Hz. At the undulator this train has a duration of 1 ms but consists of 11 315 single bunches of length 180 fs. The SASE process (self-amplified stimulated emission) inside the undulator subdivides the single bunches further, so that the emerging X-rays come in bursts of coherent radiation with an average length of 0.1 fs. In the following we shall consider one such isolated pulse.

For the development of X-ray optics for such a beam it is interesting to know the effect of crystal reflection. The reflection of short X-ray pulses has been investigated by several authors, among them Wark & Lee (1999), Shastri *et al.* (2001) and Graeff (2002). In the latter two papers analytic approaches were attempted whereas Wark & Lee carried out a simulation. Besides the Bragg case, symmetric Laue geometry was studied. Both authors found that in the Laue case the time duration of the pulse after diffraction is $2(T/c)\sin^2\theta/\cos\theta$, where T is the thickness of the crystal, θ is the Bragg angle and c is the speed of light. However, in the latter paper the propagation of the beam behind the crystal was explicitly given. On the basis of qualitative considerations one could then expect that the asymmetric case could reduce the time duration of the pulse and also modify the geometry of the pulse after diffraction. This was a strong motivation to study the asymmetric Laue case. Furthermore, this work gave the opportunity to present a somewhat different treatment which casts a new light on the problem. Naturally both calculations lead to the same final results.

2. Modelling a short X-ray pulse

The SASE process results in an almost parallel photon beam with a diameter of 50 μm (r.m.s.) at the end of the undulator. Let us characterize its direction by the unit vector \mathbf{u} . The monochromator is situated at a distance of about 800 m from the undulator and this is the domain of Fraunhofer diffraction which induces a divergence of 2 μrad for a wavelength of 1 \AA . This is very small compared with the 15 μrad width of a 111 diamond rocking curve. Since the transverse spread of the photon beam is about 1.6 mm at this distance, one can consider the incident pulse as a plane wave. We consider here a single coherent pulse of duration 0.1 fs (but still 300 periods) as explained above. The electric field can then be approximated by $\mathbf{E}_0^a\delta(t - \mathbf{ur}/c)$. The origin of coordinates O has been taken in the plane normal to \mathbf{u} where the pulse stands at $t = 0$ (Fig. 1). The small duration of the pulse leads to a frequency spectrum of the order of 10^{16} s^{-1} which for a central frequency of $3 \times 10^{18} \text{ s}^{-1}$ gives $\Delta\nu/\nu = 0.3 \times 10^{-2}$, which is very broad compared with the frequency range of the order of 10^{-5} where diffraction occurs. This justifies *a posteriori* the δ -function which by Fourier transform gives an infinite sum of plane waves with all frequencies ν and corresponding wave vectors $\mathbf{K}_0 = (\nu/c)\mathbf{u}$,

$$\begin{aligned} \mathbf{E}_0^a\delta(t - \mathbf{ur}/c) &= (\mathbf{E}_0^a/2\pi) \int \exp i\omega(\mathbf{ur}/c - t) d\omega \\ &= \mathbf{E}_0^a \int \exp 2\pi i\nu(\mathbf{ur}/c - t) d\nu. \end{aligned} \quad (1)$$

In fact the incident pulse has a very small but definite duration and the frequency spectrum is not really infinite. Thereby we avoid problems with the validity of the two-wave solutions we will adopt later; for instance, the assumption that only two waves are dominant in the crystal or that the curvature of the asymptotes of the dispersion surface is neglected.

In the following we consider that the crystal is at exact Bragg incidence for a given frequency. For any other frequency the crystal is no longer at exact Bragg incidence since the Bragg angle varies with frequency, and we first calculate the reflected and transmitted beams inside the crystal (§3) and then after the crystal (§4) for this frequency. The summation over all frequencies is performed in the second part of §4 and leads to functions of position and time. The resulting transmitted and diffracted signals passing through a given position after the crystal are analysed as a function of time in §5. It is shown that the diffracted signal is no longer a δ -function but has a duration whose value is proportional to the thickness of the crystal. The shape of the snapshot of the reflected and transmitted signal is analysed in §6.

3. Wavefields in the crystal

The crystal is adjusted so that the angle θ between \mathbf{u} and the reflecting plane is the sum of the exact Bragg angle $\theta_{B,c}$ for a given frequency ν_c .

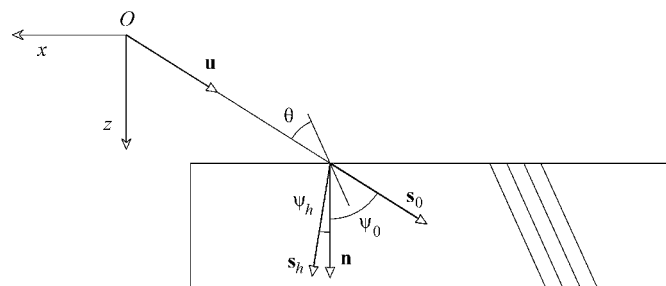


Figure 1 Geometry in real space of an asymmetric Laue-case diffraction. Oz is normal to the crystal surface.

$$E_0(\mathbf{r}) = E_0^a \left[C_0^{(1)} \exp 2\pi i \delta^{(1)} T + C_0^{(2)} \exp 2\pi i \delta^{(2)} T \right] \exp 2\pi i \mathbf{K}_0 \mathbf{r} = E_0^a V(\eta) \exp 2\pi i \mathbf{K}_0 \mathbf{r}, \quad (11)$$

$$E_h(\mathbf{r}) = E_0^a \left[C_h^{(1)} \exp 2\pi i \delta^{(1)} T + C_h^{(2)} \exp 2\pi i \delta^{(2)} T \right] \times \exp 2\pi i \mathbf{K}_h \mathbf{r}_s \exp 2\pi i \mathbf{K}'_h (\mathbf{r} - \mathbf{r}_s) = E_0^a R(\eta) \exp 2\pi i \mathbf{K}_h \mathbf{r}_s \exp 2\pi i \mathbf{K}'_h (\mathbf{r} - \mathbf{r}_s), \quad (12)$$

where

$$V(\eta) = M \left[\cos A(1 + \eta^2)^{1/2} - i\eta(1 + \eta^2)^{-1/2} \sin A(1 + \eta^2)^{1/2} \right] \exp i\eta A, \quad (13)$$

$$R(\eta) = N(1 + \eta^2)^{-1/2} \sin A(1 + \eta^2)^{1/2} \exp i\eta A, \quad (14)$$

where

$$M = \exp \pi i k \chi_0 T / \gamma_0,$$

$$N = i[(\chi_h \chi_{\bar{h}})^{1/2} / \chi_h] (\gamma_0 / \gamma_h)^{1/2} \exp \pi i k \chi_0 T / \gamma_0$$

and

$$A = \pi T / \Lambda_L.$$

Considering now the dependence in time t (we still discuss a single incident wave with a given frequency ν) one obtains

$$E_0(\mathbf{r}, t, \nu) = E_0^a V[\eta(\nu)] \exp 2\pi i \mathbf{K}_0 \mathbf{r} \exp -2\pi i \nu t, \quad (15)$$

$$E_h(\mathbf{r}, t, \nu) = E_0^a R[\eta(\nu)] \exp 2\pi i \mathbf{K}_h \mathbf{r}_s \exp 2\pi i \mathbf{K}'_h (\mathbf{r} - \mathbf{r}_s) \exp -2\pi i \nu t. \quad (16)$$

Writing $\mathbf{K}_0 = \mathbf{K}_{0,c} + \Delta\mathbf{K}_0$, $\mathbf{K}_h = \mathbf{K}_{h,c} + \Delta\mathbf{K}_h$, $\mathbf{K}'_h = \mathbf{K}'_{h,c} + \Delta\mathbf{K}'_h$ and $\nu = \nu_c + \Delta\nu$, we obtain

$$E_0(\mathbf{r}, t, \nu) = E_0^a V[\eta(\nu)] \exp 2\pi i \mathbf{K}_{0,c} \mathbf{r} \exp -2\pi i \nu_c t \times \exp 2\pi i \Delta\mathbf{K}_0 \mathbf{r} \exp -2\pi i \Delta\nu t, \quad (17)$$

$$E_h(\mathbf{r}, t, \nu) = E_0^a R[\eta(\nu)] \exp 2\pi i \mathbf{K}_{h,c} \mathbf{r}_s \exp 2\pi i \mathbf{K}'_{h,c} (\mathbf{r} - \mathbf{r}_s) \times \exp -2\pi i \nu_c t \exp 2\pi i \Delta\mathbf{K}_h \mathbf{r}_s \times \exp 2\pi i \Delta\mathbf{K}'_h (\mathbf{r} - \mathbf{r}_s) \exp -2\pi i \Delta\nu t. \quad (18)$$

Putting all constant factors related to the central wave into the factors E_0 and E_h we may rewrite

$$E_0(\mathbf{r}, t, \nu) = E_0 V[\eta(\nu)] \exp 2\pi i \Delta\mathbf{K}_0 \mathbf{r} \exp -2\pi i \Delta\nu t, \quad (19)$$

$$E_h(\mathbf{r}, t, \nu) = E_h R[\eta(\nu)] \exp 2\pi i \Delta\mathbf{K}_h \mathbf{r}_s \exp 2\pi i \Delta\mathbf{K}'_h (\mathbf{r} - \mathbf{r}_s) \times \exp -2\pi i \Delta\nu t. \quad (20)$$

Finally the electric field is obtained by integration of (19) and (20) on all values of ν ,

$$E_0(\mathbf{r}, t) = E_0 \int V[\eta(\Delta\nu)] \exp 2\pi i (\Delta\mathbf{K}_0 \mathbf{r} - \Delta\nu t) d\Delta\nu, \quad (21)$$

$$E_h(\mathbf{r}, t) = E_h \int R[\eta(\Delta\nu)] \exp 2\pi i [\Delta\mathbf{K}_h \mathbf{r}_s + \Delta\mathbf{K}'_h (\mathbf{r} - \mathbf{r}_s) - \Delta\nu t] d\Delta\nu. \quad (22)$$

To perform this integration one needs to express $\Delta\mathbf{K}_0$, $\Delta\mathbf{K}_h$ and $\Delta\mathbf{K}'_h$ as functions of $\Delta\nu$ (or $\Delta k = \Delta\nu/c$) and then $\Delta\nu$ (or Δk) as a function of η with equation (4).

In Fig. 2 for the frequency ν_c the Ewald spheres in the air intersect at the Laue point L_c and the incident wavevector is $\mathbf{K}_{0,c} = \mathbf{L}_c \mathbf{O} = k_c \mathbf{u}$. For a frequency $\nu = \nu_c + \Delta\nu$ and a corresponding wavevector length

$k = k_c + \Delta k$ they intersect at L . The incident wavevector is $\mathbf{K}_0 = \mathbf{M}\mathbf{O} = (k_c + \Delta k)\mathbf{u}$. From the definition (8) of \mathbf{K}_h , $\mathbf{K}_{h,c} = \mathbf{L}_c \mathbf{H}$ and $\mathbf{K}_h = \mathbf{M}\mathbf{H}$. The diffracted wave vectors in the air depend on η and are $\mathbf{K}'_h = \mathbf{M}'\mathbf{H}$. Then $\Delta\mathbf{K}_0 = \Delta\mathbf{K}_h = \mathbf{M}\mathbf{L}_c = \Delta k \mathbf{u}$ and $\Delta\mathbf{K}'_h = \mathbf{M}'\mathbf{L}_c$ which are calculated now.

\mathbf{r}_s joins the origin to an arbitrary point on the exit surface. Let us call it O' . $\mathbf{u}\mathbf{r}_s = l_0$ where l_0 is the distance between the incident wave front in O and O' (Fig. 3). Correspondingly, we define $l = \mathbf{u}\mathbf{r}$. Finally,

$$\Delta\mathbf{K}_0 \mathbf{r} = \Delta k l, \quad (23)$$

$$\Delta\mathbf{K}_h \mathbf{r}_s = \Delta k l_0. \quad (24)$$

Simple calculations show that

$$\Delta\mathbf{K}'_h = \mathbf{M}'\mathbf{L}_c = \Delta k \{ -\sin \psi_0 \mathbf{u}_x + [(1 + \sin \psi_0 \sin \psi_h) / \gamma_h] \mathbf{u}_z \}, \quad (25)$$

where \mathbf{u}_x and \mathbf{u}_z are unit vectors parallel to Ox and Oz defined in Fig. 1. The positive direction of the x axis is chosen to the left of the figure.

Let us define a coordinate system $O'x'y'z'$ parallel to $Oxyz$ (Fig. 3) with the origin O' on the exit surface as defined above. Replacing Δk as a function of η , equation (21) becomes

$$E_0(\mathbf{r}, t) = E_0' \int V(\eta) \exp \pi i [\eta \gamma_h / (\Lambda_L \sin^2 \theta_B)] (l - ct) d\eta, \quad (26)$$

and equation (22) for the diffracted beam becomes

$$E_h(\mathbf{r}, t) = E_h' \int R(\eta) \exp \pi i [\eta \gamma_h / (\Lambda_L \sin^2 \theta_B)] \times \{ l_0 - ct - x' \sin \psi_0 + z' [(1 + \sin \psi_0 \sin \psi_h) / \gamma_h] \} d\eta. \quad (27)$$

The constants in front are modified and now include the transformation factors when going to different integration variables. For convenience we define the variables

$$\xi_0 = A + [\pi \gamma_h / (\Lambda_L \sin^2 \theta)] (l - ct), \quad (28)$$

$$\xi_h = A + [\pi \gamma_h / (\Lambda_L \sin^2 \theta)] \{ l_0 - ct - x' \sin \psi_0 + z' [(1 + \sin \psi_0 \sin \psi_h) / \gamma_h] \}.$$

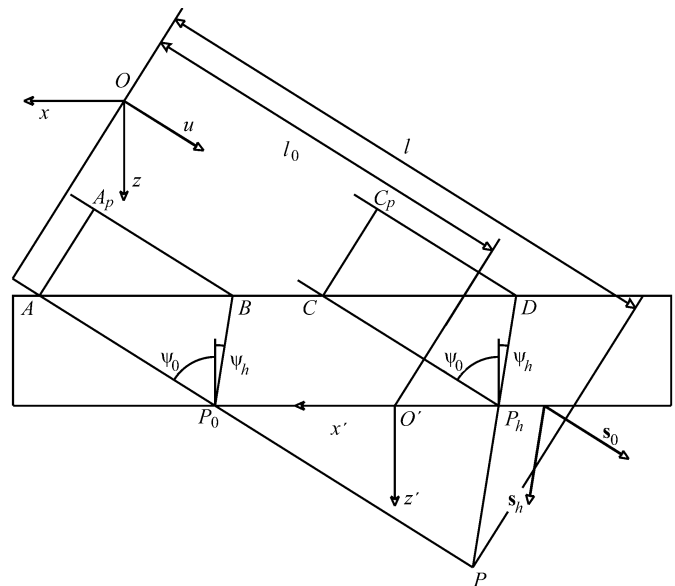


Figure 3

Relevant points to measure a signal at P . This point receives intensity from P_0 via the 0-beam, which in turn receives intensity from the reverse Borrmann triangle ABP_0 . The same happens via the h -beam. The reverse Borrmann triangle is in this case CDP_h .

Then with the help of equations (13), (14), (26), (27) and (28) we may write the expressions for the transmitted and the diffracted pulse behind the crystal,

$$\begin{aligned} E_0(\mathbf{r}, t) &= E_0''G(\xi_0), \\ E_h(\mathbf{r}, t) &= E_h''I(\xi_h), \end{aligned} \quad (29)$$

with

$$\begin{aligned} G(\xi_0) &= \int [\cos A(1 + \eta^2)^{1/2} - i\eta(1 + \eta^2)^{-1/2} \sin A(1 + \eta^2)^{1/2}] \\ &\quad \times \exp i\xi_0\eta \, d\eta, \\ I(\xi_h) &= \int \{[\sin A(1 + \eta^2)^{1/2}]/(1 + \eta^2)^{1/2}\} \exp i\xi_h\eta \, d\eta. \end{aligned} \quad (30)$$

The integrals are evaluated in Appendix B [equations (57) and (62), respectively]. So we finally have explicitly the phase factors from the central wave,

$$\begin{aligned} E_0(\mathbf{r}, t) &= E_0'''[(A + \xi_0)/(A - \xi_0)]^{1/2} J_1((A^2 - \xi_0^2)^{1/2}) \\ &\quad \times \exp 2\pi i(\mathbf{K}_{0,c}\mathbf{r} - \nu_c t), \end{aligned} \quad (31)$$

$$E_h(\mathbf{r}, t) = E_h'''J_0((A^2 - \xi_h^2)^{1/2}) \exp 2\pi i(\mathbf{K}'_{h,c}\mathbf{r} - \nu_c t), \quad (32)$$

where all irrelevant constants are included in E_0''' and E_h''' . The expressions are limited to domains

$$\begin{aligned} -(2T \sin^2 \theta)/\gamma_h &< l - ct < 0 && \text{0-beam,} \\ -(2T \sin^2 \theta)/\gamma_h &< l_0 - ct - x' \sin \psi_0 + \\ &z'[(1 + \sin \psi_0 \sin \psi_h)/\gamma_h] < 0 && \text{h-beam.} \end{aligned} \quad (33)$$

Outside these domains the electric field values vanish.

The transmitted and diffracted ‘pulse’ is no longer a δ -pulse but is spread in time and position inside limited domains. Of course, the measured signal is the intensity which is easily obtained from equations (31) and (32) by taking the square moduli,

$$\begin{aligned} I_0(\mathbf{r}, t) &= |E_0'''|^2 \left[\left[(A + \xi_0)/(A - \xi_0) \right]^{1/2} J_1((A^2 - \xi_0^2)^{1/2}) \right]^2, \\ I_h(\mathbf{r}, t) &= |E_h'''|^2 J_0^2((A^2 - \xi_h^2)^{1/2}). \end{aligned} \quad (34)$$

The extensions of the domains given in equations (33) are not influenced.

Let us now interpret in detail equations (33) which define the domains where the amplitudes E_0 and E_h do not vanish.

5. Signal at a given point behind the crystal

The two domains for the 0- and h -direction overlap close to the exit surface of the crystal. This situation resembles the well known standing-wave patterns, but as the domains move with the speed of light this overlap region is not stationary but moves along the exit surface of the crystal.

To avoid complications we choose a point well behind the overlap region. At this point $P = (x', z')$ (see Fig. 3) the pulse in the 0-direction arrives first. The incident pulse passes through O at $t = 0$ and its arrival time is

$$t_{0,1} = l/c. \quad (35)$$

From condition (33) one sees that the pulse in the 0-direction lasts until

$$t_{0,2} = (2T \sin^2 \theta)/c\gamma_h + l/c. \quad (36)$$

Hence the pulse duration is

$$\Delta t = (2T \sin^2 \theta)/c\gamma_h, \quad (37)$$

which is understood easily as the phase front of the pulse travels at the speed of light between two extreme paths, one being AP_0P and the other A_pBP_0P . The path difference is easily verified to be $c\Delta t$.

The arrival time of the diffracted pulse at P is

$$t_{h,1} = l_0/c - x'(\sin \psi_0)/c + z'(1 + \sin \psi_0 \sin \psi_h)/c\gamma_h. \quad (38)$$

It lasts until

$$\begin{aligned} t_{h,2} &= l_0/c - x'(\sin \psi_0)/c + z'(1 + \sin \psi_0 \sin \psi_h)/c\gamma_h \\ &\quad + (2T \sin^2 \theta)/c\gamma_h, \end{aligned} \quad (39)$$

which results in the same pulse duration as given in (37), as the path difference between CP_h and C_pDP_h is the same as that between AP_0 and A_pBP_0 .

6. Signal at a given time

Now we look at a snapshot of the intensity distribution behind the crystal. Let us consider for example the time t when the beginning of the signal arrives at B (see Fig. 6). We expect two stripes, one for the transmitted pulse and one for the diffracted pulse. The front borders of both stripes meet at B , the rear borders at G .

The domain of the 0-beam is derived from condition (33) which refers to l . Lines of equal intensity are perpendicular to the incidence direction and the extreme values are separated by Δl such that

$$\Delta l = (2T \sin^2 \theta)/\gamma_h. \quad (40)$$

The distance between B and G is

$$\overline{BG} = \Delta l / \sin \psi_0 = 2T \sin^2 \theta / (\gamma_h \sin \psi_0). \quad (41)$$

The domain of the h -beam where the electric field is different from zero is, from condition (33), a function of

$$l_0 - ct - x' \sin \psi_0 + z'[(1 + \sin \psi_0 \sin \psi_h)/\gamma_h],$$

which is constant along lines parallel to

$$z' = x'[(\sin \psi_0 \cos \psi_h)/(1 + \sin \psi_0 \sin \psi_h)] = x' \tan \beta. \quad (42)$$

The geometrical construction of such a line is simple and easy to understand if one considers as above the wave fields which propagate along the margins of the Borrmann triangle at the speed of light. The incident pulse enters the crystal at two points, A and A' for example in Fig. 4, corresponding to a wave front $A'A'_p$. Considering only the propagation along direction \mathbf{s}_0 , the wave incident at A exits the crystal at B and that incident at A' exits at B' . The waves in B and B' are not in phase because of the beam paths difference A'_pA . The reflected waves are in phase at point B and point B'_h defined along the reflected direction issued from B' by the condition $B'B'_h = A'_pA$. It can be shown that the angle between BB'_h and the exit surface BB' is equal to the angle β defined above.

The intensity of the diffracted signal is confined between two such parallel lines: one passing through B and the other through a point G already given above with the 0-domain. Fig. 5 shows an independent method of finding the location of G . After constructing the angle β and the first line through B (Fig. 4), the Borrmann triangle ABC is extended to the isosceles triangle ABC_h . A parallel line to BD is drawn through C_h . The intersection of this line with the back of the crystal gives G . It can be checked that $EF = CC_h$.

In order to interpret this result let us consider Fig. 6 where the Borrmann triangle ABC has been extended to the isosceles triangle ABC_h . The δ -pulse is a plane wave (at a given time the signal spreads over all the plane perpendicular to \mathbf{u}) but owing to its temporal

structure it contains all the frequencies. As a result, when the δ -pulse arrives at A at time $t_0 = \overline{OA}/c$ all the wave fields are excited and spread inside the Borrmann triangle ABC with a group velocity v_g which depends on the direction of propagation. The group velocity is equal to $c \cos \theta / \cos \varphi$, where φ is the angle between the direction of propagation of the wavefield and the trace of the reflecting planes. The wavefields arrive at the exit surface at different times and then decompose outside the crystal into reflected and transmitted waves propagating at c , the speed of light. It can be shown that at time $t = t_0 + T/c\gamma_0$, when the wave field which propagates along the margin AB of the Borrmann triangle (with speed c) arrives at the exit surface at B , the different reflected beams which have propagated inside the crystal with speed v_g and outside the crystal with speed c spread over the line BC_h (and the transmitted beams over BC_0).

Let us consider now the wave fields issued of the plane wave pulse impinging the crystal entrance surface at point A' at a later time. The pattern is shifted to the right. Equivalent points on the border of each domain are marked by circles. They move at the speed of light in the corresponding direction.

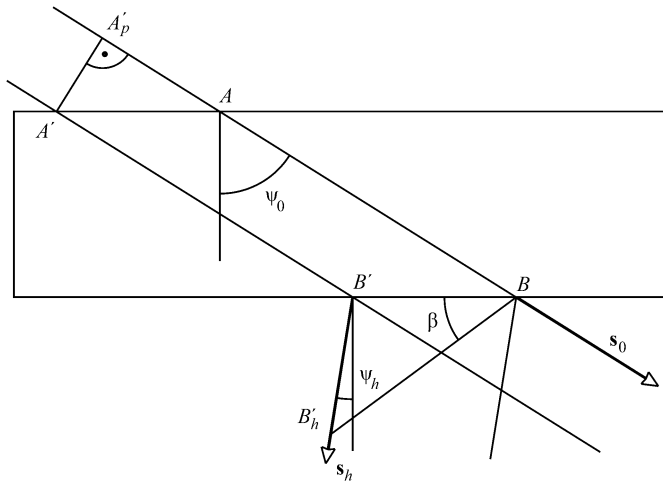


Figure 4
Finding the angle β , the inclination of the h -domain with respect to the crystal (see text).

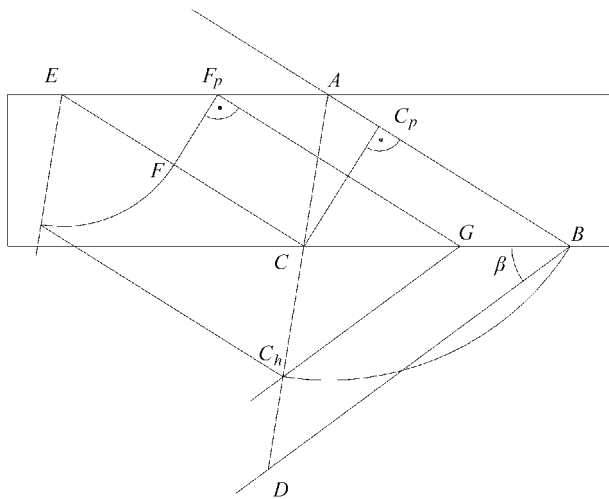


Figure 5
Constructing the point G which defines the second boundary of the h -domain (see text).

The temporal evolution of the diffracted stripe may be seen as a slower movement in the normal direction. That speed is its group velocity, different from c because of the variation of the direction of the diffracted wave vectors as a function of the frequency of the wave. The group velocity may easily be deduced from the width of the stripe $\overline{BG} \sin \beta$ [equations (41) and (42)] and the duration of the pulse [equation (37)],

$$v_g = c\gamma_h(1 + 2 \sin \psi_0 \sin \psi_h + \sin^2 \psi_0)^{-1/2}. \quad (43)$$

A numerical example would be for a diamond 111-reflection in the symmetric Laue case, $0.89c$.

In practice the lateral size of the incident pulse is limited and there are some lateral edge effects which are not taken into account here.

It is worthwhile noticing that the variation of the intensity across the transmitted and diffracted stripes as given in formulae (34) is at least formally identical to the intensity variation of the beams if a monochromatic spherical wave impinges the crystal with the same central frequency. In both cases a dimensionless coordinate varying from 0 to 1 is used. However, in the case of a spherical wave this coordinate covers the base of the Borrmann triangle and the diffracted beam has the direction of s_h , whereas in the case of a δ -pulse the coordinate is confined to the stripes. Note that in general points C and G in Fig. 5 do not coincide.

7. Conclusions

Analytic expressions for the diffraction of a short X-ray pulse from an asymmetric Laue-case crystal have been deduced. They resemble the well known Pendellösung solutions for an incident spherical wave. The incident short pulse is no longer short after diffraction but extended over a time

$$\Delta t = (2T \sin^2 \theta) / c\gamma_h,$$

and depends on three quantities:

- (i) The thickness T of the crystal which is of the order of $100 \mu\text{m}$, if mechanical means like diamond saws are used, but can go down to several μm if physicochemical processes from the fabrication of electronic devices are used.

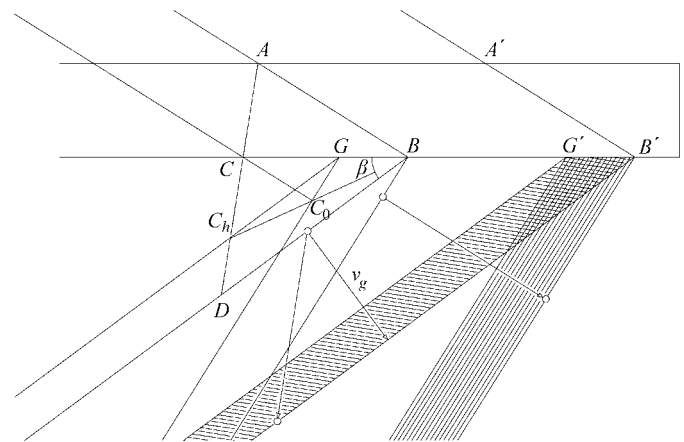


Figure 6
The intensity distribution at two different times, when the pulse arrives at B and B' . The propagation of equivalent points is indicated by circles. To emphasize the different orientation of phase fronts they are indicated in the domains when the pulse arrives at B' . The overlapping area of the transmitted and reflected beams is clearly visible. For clarity the corresponding areas at B are not hatched.

(ii) The Bragg angle. The choice is limited by the diffraction mechanism. In order to shorten the pulse, an order of reflection as low as possible should be selected. For example, for a diamond 111-reflection and 1 Å wavelength, $\theta = 14.08^\circ$.

(iii) The asymmetry of the crystal. Obviously the optimal choice is $\gamma_h = 1$, which means that the diffracted beam leaves the crystal perpendicularly. Taking the optimal values of all three parameters together, several fs can be achieved (*e.g.* for $T = 10 \mu\text{m}$, $\Delta t = 4 \text{ fs}$, for $T = 100 \mu\text{m}$, $\Delta t = 40 \text{ fs}$).

At a given time the transmitted and diffracted beams spread over stripes. The intensity across the stripe varies (as Bessel functions) exactly as the intensity along the exit surface of a crystal in Laue diffraction for an incident spherical wave. It is not really surprising since the ultrashort pulse leads, by Fourier transform, to a wide range of frequencies resulting in excitation of the whole dispersion surface analogous to the case of a monochromatic spherical wave. As has been shown, the margins of the stripes are associated with the wavefields propagating along the incident and reflected directions, respectively, and corresponding in the integral to large values of the modulus of the η parameter.

Finding an analytic result was possible using several assumptions which were reasonable and are worthwhile reviewing. First, the incident pulse must be much shorter than the response time of the crystal finally deduced. This is fulfilled easily since the response time is at least several fs to be compared with 0.1 fs. Second, the divergence of the incident pulse was assumed to be zero. The divergence is of the order of $2 \mu\text{rad}$ directly associated with the lateral width of the beam at the exit of the undulator. It is very small compared with the width of the rocking curve and would only somewhat blur the fringes across the stripe. Third, the curvature of the asymptotes of the dispersion surface was neglected. This would influence large η values which contribute to the margins of the Bessel functions. On the other hand, in reality the finite pulse width strongly suppresses large frequency deviations (hence large η values).

Finally, let us consider the transmitted and diffracted beams given in equations (31) and (32) which are of the form $A(\mathbf{r}, t) \exp 2\pi i(\mathbf{k}_c \mathbf{r} - \nu_c t)$. On first glance they look like plane waves because of the factor $\exp 2\pi i(\mathbf{k}_c \mathbf{r} - \nu_c t)$, but one has to also consider the spatial dependence of the factor $A(\mathbf{r}, t)$. The Fourier transform of the whole function requires the region around \mathbf{k}_c to be occupied in k -space. For the transmitted beam this factor is a function of $l - ct$ where l is a distance parallel to \mathbf{k}_c . Consequently no further divergence is added and one obtains a ‘plane’ wave and, as noticed above, the stripe is normal to the \mathbf{k}_c vector. On the contrary the reflected beam is not a non-divergent wave; each frequency gives rise to a different reflected wavevector and the stripe is not normal to \mathbf{k}_c . Its propagation speed in the direction normal to the stripe is smaller than the speed of light. Hence we have an electromagnetic field distribution which travels in a vacuum slower than the speed of light.

By choosing the appropriate asymmetry angle one could not only shorten the pulse but also evoke another interesting situation. By setting $\psi = 0$, *i.e.* making the incident beam impinge normal to the crystal surface, it follows from equation (42) that the diffracted stripe leaves the crystal parallel to the rear surface. As its group velocity is still lower than the speed of light, namely $v_g = c \cos 2\theta$, its separation from the direct pulse depends on the distance to the crystal. A sample behind the crystal would first be hit by the direct pulse and then by its echo, independent of the lateral position. Unfortunately this phenomenon occurs only in regions close to the crystal where the reflected and the transmitted beam superimpose and the lateral width of this common area decreases with the distance from the crystal, in practical situations within a few millimeters.

APPENDIX A

Amplitudes at the crystal surfaces

The aim of this Appendix is to prove the validity of the form of the diffracted wave given in (7) which introduces a fictive incident diffracted wave. This is not done in standard books on dynamical theory which add this wave as if it was evident.

One incident plane wave $E_0^a \exp 2\pi i \mathbf{K}_0 \mathbf{r}$ gives rise to two wavefields in the crystal,

$$\begin{aligned} E^{(1)} &= E_0^{(1)} \exp 2\pi i \mathbf{k}_0^{(1)} \mathbf{r} + E_h^{(1)} \exp 2\pi i \mathbf{k}_h^{(1)} \mathbf{r}, \\ E^{(2)} &= E_0^{(2)} \exp 2\pi i \mathbf{k}_0^{(2)} \mathbf{r} + E_h^{(2)} \exp 2\pi i \mathbf{k}_h^{(2)} \mathbf{r}, \end{aligned}$$

where the wave vectors $\mathbf{k}_0^{(1)}$, $\mathbf{k}_0^{(2)}$, $\mathbf{k}_h^{(1)}$, $\mathbf{k}_h^{(2)}$ are determined by the continuity of their tangential components.

In order to express the different waves $E_0^{(j)} \exp 2\pi i \mathbf{k}_0^{(j)} \mathbf{r}$ and $E_h^{(j)} \exp 2\pi i \mathbf{k}_h^{(j)} \mathbf{r}$ excited by a given incident plane wave one has to apply boundary conditions at the entrance surface for the incident and reflected waves which gives

$$\begin{aligned} E_0^a \exp 2\pi i \mathbf{K}_0 \mathbf{r}_e &= E_0^{(1)} \exp 2\pi i \mathbf{k}_0^{(1)} \mathbf{r}_e + E_0^{(2)} \exp 2\pi i \mathbf{k}_0^{(2)} \mathbf{r}_e, \\ 0 &= E_h^{(1)} \exp 2\pi i \mathbf{k}_h^{(1)} \mathbf{r}_e + E_h^{(2)} \exp 2\pi i \mathbf{k}_h^{(2)} \mathbf{r}_e, \end{aligned} \quad (44)$$

where \mathbf{r}_e is any vector with its end point at the entrance surface.

This system is easily solved by multiplying both sides of the last equation by $\exp -2\pi i \mathbf{K}_h \mathbf{r}_e$, where $\mathbf{K}_h = \mathbf{K}_0 + \mathbf{h}$, in order to obtain identical exponential factors for $E_0^{(1)}$ and $E_h^{(1)}$ and for $E_0^{(2)}$ and $E_h^{(2)}$, since

$$\begin{aligned} \mathbf{K}_h - \mathbf{k}_h^{(1)} &= \mathbf{K}_0 - \mathbf{k}_0^{(1)}, \\ \mathbf{K}_h - \mathbf{k}_h^{(2)} &= \mathbf{K}_0 - \mathbf{k}_0^{(2)}. \end{aligned} \quad (45)$$

One obtains the following system of two equations describing the boundary conditions at the entrance surface,

$$\begin{aligned} E_0^a &= E_0^{(1)} \exp 2\pi i [\mathbf{k}_0^{(1)} - \mathbf{K}_0] \mathbf{r}_e + E_0^{(2)} \exp 2\pi i [\mathbf{k}_0^{(2)} - \mathbf{K}_0] \mathbf{r}_e, \\ 0 &= E_h^{(1)} \exp 2\pi i [\mathbf{k}_h^{(1)} - \mathbf{K}_h] \mathbf{r}_e + E_h^{(2)} \exp 2\pi i [\mathbf{k}_h^{(2)} - \mathbf{K}_h] \mathbf{r}_e. \end{aligned} \quad (46)$$

Introducing the amplitude ratios $\xi^{(1)} = E_h^{(1)}/E_0^{(1)}$ and $\xi^{(2)} = E_h^{(2)}/E_0^{(2)}$ and using (45) we obtain a system of two unknowns and two equations,

$$\begin{aligned} E_0^a &= E_0^{(1)} \exp 2\pi i [\mathbf{k}_0^{(1)} - \mathbf{K}_0] \mathbf{r}_e + E_0^{(2)} \exp 2\pi i [\mathbf{k}_0^{(2)} - \mathbf{K}_0] \mathbf{r}_e, \\ 0 &= \xi^{(1)} E_0^{(1)} \exp 2\pi i [\mathbf{k}_0^{(1)} - \mathbf{K}_0] \mathbf{r}_e + \xi^{(2)} E_0^{(2)} \exp 2\pi i [\mathbf{k}_0^{(2)} - \mathbf{K}_0] \mathbf{r}_e, \end{aligned} \quad (47)$$

which is easily solved.

Consequently the amplitudes of the diffracted wavefields are

$$\begin{aligned} E_0^{(1)} &= \{\xi^{(2)}/[\xi^{(2)} - \xi^{(1)}]\} E_0^a \exp 2\pi i [\mathbf{K}_0 - \mathbf{k}_0^{(1)}] \mathbf{r}_e, \\ E_0^{(2)} &= \{-\xi^{(1)}/[\xi^{(2)} - \xi^{(1)}]\} E_0^a \exp 2\pi i [\mathbf{K}_0 - \mathbf{k}_0^{(2)}] \mathbf{r}_e, \\ E_h^{(1)} &= \{\xi^{(1)} \xi^{(2)}/[\xi^{(2)} - \xi^{(1)}]\} E_0^a \exp 2\pi i [\mathbf{K}_h - \mathbf{k}_h^{(1)}] \mathbf{r}_e, \\ E_h^{(2)} &= \{-\xi^{(2)} \xi^{(1)}/[\xi^{(2)} - \xi^{(1)}]\} E_0^a \exp 2\pi i [\mathbf{K}_h - \mathbf{k}_h^{(2)}] \mathbf{r}_e, \end{aligned}$$

or

$$\begin{aligned} E_0^{(j)} &= E_0^a C_0^{(j)} \exp 2\pi i [\mathbf{K}_0 - \mathbf{k}_0^{(j)}] \mathbf{r}_e, \\ E_h^{(j)} &= E_0^a C_h^{(j)} \exp 2\pi i [\mathbf{K}_h - \mathbf{k}_h^{(j)}] \mathbf{r}_e. \end{aligned} \quad (48)$$

Dynamical theory [see for example Kato (1974) and Authier (2001)] gives the coefficients as a function of the incidence parameter [equation (2)],

$$\begin{aligned} C_0^{(j)} &= [(\eta^2 + 1)^{1/2} \mp \eta] / [2(\eta^2 + 1)^{1/2}], \\ C_h^{(j)} &= \pm [(\chi_h \chi_{\bar{h}})^{1/2} / 2\chi_h] (\gamma_0 / \gamma_h)^{1/2} (\eta^2 + 1)^{-1/2}. \end{aligned} \quad (49)$$

The upper sign holds for $j = 1$ and the lower one for $j = 2$.

The four waves inside the crystal are

$$\begin{aligned} E_0^{(j)}(\mathbf{r}) &= E_0^{(j)} \exp 2\pi i \mathbf{k}_0^{(j)} \mathbf{r} \\ &= E_0^a C_0^{(j)} \exp 2\pi i [\mathbf{K}_0 - \mathbf{k}_0^{(j)}] \mathbf{r}_e \exp 2\pi i \mathbf{k}_0^{(j)} \mathbf{r} \\ &= E_0^a C_0^{(j)} \exp 2\pi i \mathbf{K}_0 \mathbf{r}_e \exp 2\pi i \mathbf{k}_0^{(j)} (\mathbf{r} - \mathbf{r}_e), \end{aligned} \quad (50)$$

$$\begin{aligned} E_h^{(j)}(\mathbf{r}) &= E_h^{(j)} \exp 2\pi i \mathbf{k}_h^{(j)} \mathbf{r} \\ &= E_0^a C_h^{(j)} \exp 2\pi i [\mathbf{K}_h - \mathbf{k}_h^{(j)}] \mathbf{r}_e \exp 2\pi i \mathbf{k}_h^{(j)} \mathbf{r} \\ &= E_0^a C_h^{(j)} \exp 2\pi i \mathbf{K}_h \mathbf{r}_e \exp 2\pi i \mathbf{k}_h^{(j)} (\mathbf{r} - \mathbf{r}_e), \end{aligned} \quad (51)$$

which can be arranged as

$$E_0^{(j)}(\mathbf{r}) = E_0^a C_0^{(j)} \exp 2\pi i [\mathbf{k}_0^{(j)} - \mathbf{K}_0] (\mathbf{r} - \mathbf{r}_e) \exp 2\pi i \mathbf{K}_0 \mathbf{r}, \quad (52)$$

$$E_h^{(j)}(\mathbf{r}) = E_0^a C_h^{(j)} \exp 2\pi i [\mathbf{k}_h^{(j)} - \mathbf{K}_h] (\mathbf{r} - \mathbf{r}_e) \exp 2\pi i \mathbf{K}_h \mathbf{r}. \quad (53)$$

The last arrangement leads directly to the boundary conditions at the back of the crystal. At a given point \mathbf{r}_s at the exit surface of a crystal of thickness T ,

$$E_0^{(j)}(\mathbf{r}_s) = E_0^a C_0^{(j)} \exp 2\pi i \delta^{(j)} T \exp 2\pi i \mathbf{K}_0 \mathbf{r}_s, \quad (54)$$

$$E_h^{(j)}(\mathbf{r}_s) = E_0^a C_h^{(j)} \exp 2\pi i \delta^{(j)} T \exp 2\pi i \mathbf{K}_h \mathbf{r}_s, \quad (55)$$

with

$$\begin{aligned} \delta^{(j)} &= [\mathbf{k}_0^{(j)} - \mathbf{K}_0] \mathbf{n} = [\mathbf{k}_h^{(j)} - \mathbf{K}_h] \mathbf{n} \\ &= k\chi_0 / 2\gamma_0 + \eta / 2\Lambda_L \pm (\eta^2 + 1)^{1/2} / 2\Lambda_L, \end{aligned} \quad (56)$$

where the latter again comes from dynamical theory.

APPENDIX B

Evaluation of integrals over η

In *Table of Integrals, Series and Products* (Gradshteyn & Ryzhik, 1980) one finds

$$\begin{aligned} I(\xi_h) &= \int \left\{ [\sin A(1 + \eta^2)^{1/2}] / (1 + \eta^2)^{1/2} \right\} \exp i\eta \xi_h \, d\eta \\ &= \pi J_0((A^2 - \xi_h^2)^{1/2}) \quad |\xi_h| < A, \end{aligned} \quad (57)$$

and zero outside this domain. $J_0(z)$ is the Bessel function of order zero.

For the determination of the integral G one divides the integral into two parts,

$$G(\xi_0) = H(\xi_0) - K(\xi_0) \quad (58)$$

with

$$\begin{aligned} H(\xi_0) &= \int \cos A(1 + \eta^2)^{1/2} \exp i\eta \xi_0 \, d\eta, \\ K(\xi_0) &= i \int \left\{ [\eta \sin A(1 + \eta^2)^{1/2}] / (1 + \eta^2)^{1/2} \right\} \exp i\eta \xi_0 \, d\eta. \end{aligned} \quad (59)$$

Since

$$\frac{\partial I}{\partial A} = H, \quad \frac{\partial I}{\partial \xi} = K, \quad \frac{dJ_0(z)}{dz} = -J_1(z), \quad (60)$$

where $J_1(z)$ is the Bessel function of order 1, one obtains

$$\begin{aligned} H(\xi_0) &= -\pi A (A^2 - \xi_0^2)^{-1/2} J_1((A^2 - \xi_0^2)^{1/2}), \\ K(\xi_0) &= \pi \xi_0 (A^2 - \xi_0^2)^{-1/2} J_1((A^2 - \xi_0^2)^{1/2}). \end{aligned} \quad (61)$$

Finally,

$$G(\xi_0) = -\pi \left[(A + \xi_0) / (A^2 - \xi_0^2)^{1/2} \right] J_1((A^2 - \xi_0^2)^{1/2}). \quad (62)$$

References

- Authier, A. (2001). *Dynamical Theory of X-ray Diffraction*. Oxford University Press.
- DESY (1997). Report DESY 1997-048, ECFA 1997-182. DESY, Hamburg, Germany.
- DESY (2001). TESLA Technical Design Report 001-011, ECFA 2001-209. DESY, Hamburg, Germany.
- Gradshteyn, I. S. & Ryzhik, I. M. (1980). *Table of Integrals, Series and Products*. New York: Academic Press.
- Graeff, W. (2002). *J. Synchrotron Rad.* **9**, 82-85.
- Kato, N. (1968). *J. Appl. Phys.* **39**, 2225-2230.
- Kato, N. (1974). *X-ray Diffraction*, edited by V. Azaroff, ch. 4. New York: McGraw-Hill.
- Shastri, S. D., Zambianchi, P. & Mills, D. M. (2001). *J. Synchrotron Rad.* **8**, 1131-1135.
- SLAC (1998). Report SLAC-R-521, UC-414 (1998). Stanford Linear Accelerator Center, CA 94025, USA.
- Wark, J. S. & Lee, R. W. (1999). *J. Appl. Cryst.* **32**, 692-703.